Journal of
Experimental
Botany
www.jxb.oxfordjournals.org

RESEARCH PAPER

Dynamic trafficking of wheat γ-gliadin and of its structural domains in tobacco cells, studied with fluorescent protein fusions

Mathilde Francin-Allami[1],*, Amélie Saumonneau[1], Laurence Lavenant[1], Axelle Bouder[1], Imogen Sparkes[2], Chris Hawes[2] and Yves Popineau[1]

[1] UR1268 Biopolymères Interactions Assemblages, INRA, BP71627 Nantes cedex 03, France
[2] School of Life Sciences, Oxford Brookes University, Headington, Oxford OX3 0BP, UK

* To whom correspondence should be addressed. E-mail: allami@nantes.inra.fr

Abstract

Prolamins, the main storage proteins of wheat seeds, are synthesized and retained in the endoplasmic reticulum (ER) of the endosperm cells, where they accumulate in protein bodies (PBs) and are then exported to the storage vacuole. The mechanisms leading to these events are unresolved. To investigate this unconventional trafficking pathway, wheat γ-gliadin and its isolated repeated N-terminal and cysteine-rich C-terminal domains were fused to fluorescent proteins and expressed in tobacco leaf epidermal cells. The results indicated that γ-gliadin and both isolated domains were able to be retained and accumulated as protein body-like structures (PBLS) in the ER, suggesting that tandem repeats are not the only sequence involved in γ-gliadin ER retention and PBLS formation. The high actin-dependent mobility of γ-gliadin PBLS is also reported, and it is demonstrated that most of them do not co-localize with Golgi body or pre-vacuolar compartment markers. Both γ-gliadin domains are found in the same PBLS when co-expressed, which is most probably due to their ability to interact with each other, as indicated by the yeast two-hybrid and FRET-FLIM experiments. Moreover, when stably expressed in BY-2 cells, green fluorescent protein (GFP) fusions to γ-gliadin and its isolated domains were retained in the ER for several days before being exported to the vacuole in a Golgi-dependent manner, and degraded, leading to the release of the GFP 'core'. Taken together, the results show that tobacco cells are a convenient model to study the atypical wheat prolamin trafficking with fluorescent protein fusions.

Key words: endoplasmic reticulum, fluorescent proteins, *Nicotiana tabacum*, protein bodies, seed storage proteins, trafficking, wheat γ-gliadin.

Introduction

During seed development, storage proteins accumulate in the cells of the endosperm. There are two major groups of seed storage proteins: the alcohol-soluble (prolamin) storage proteins and the salt-soluble globulins (Shewry and Halford, 2002). In wheat, prolamins are classified into two major groups: the gliadins which are monomeric proteins with intramolecular disulphide bonds (α- and γ-gliadins) or without disulphide bonds (ω-gliadins), and the glutenins which are polymers possessing intra- and interchain disulphide bonds, composed of low molecular weight and high molecular weight subunits.

Prolamins are synthesized in the rough endoplasmic reticulum (ER) of endosperm cells, where they accumulate before being deposited into protein bodies (PBs) (Galili *et al.*, 1993). These PBs are derived from the ER and are transported to the storage vacuole within the endosperm cells of seeds (Parker, 1982; Parker and Hawes, 1982; Levanony *et al.*, 1992; Altschuler *et al.*, 1993). However,

the events occurring during the formation of PBs are still unclear. In the mature seeds, prolamins form a matrix around the starch grains to be used as a nitrogen source during germination. This matrix is formed along with the disappearance of PB structures (Rubin *et al.*, 1992).

A few reports indicate that wheat seed storage proteins are transported directly from the ER to the storage vacuole, bypassing the Golgi (Levanony *et al.*, 1992; Galili *et al.*, 1993; Hara-Nishimura *et al.*, 1998; Vitale and Galili 2001). This specific transport implies the formation of PBs derived from the ER, and which are directly incorporated into storage vacuoles. These results were also supported by the detection of a relatively low number of Golgi bodies in endosperm cells during the onset of storage protein synthesis and deposition (Levanony *et al.*, 1992). However, immunocytochemical studies of developing seeds detected some prolamin in Golgi bodies, suggesting trafficking of the protein via the Golgi which appears to be mainly restricted to early stages of seed development (Parker and Hawes, 1982; Galili *et al.*, 1993; Shy *et al.*, 2001; Loussert *et al.*, 2008; Tosi *et al.*, 2009).

Seed storage proteins lack the classical signals of retrieval/retention in the ER such as HDEL/KDEL, though such C-terminal extensions have been observed in a number of plant ER luminal proteins such as binding protein (BiP) and protein disulphide isomerase (PDI) (Napier *et al.*, 1992). No endogenous targeting signals were found in the case of γ-gliadin (Napier *et al.*, 1997). Currently, biological mechanisms allowing the retention of prolamins in the ER and the formation of PBs are still unknown and remain to be clarified. Several studies indicated that the N-terminal repeated domain of prolamins could be involved in the ER retention of wheat gliadin expressed in *Xenopus* oocytes (Altschuler *et al.*, 1993) or yeasts (Rosenberg *et al.*, 1993), and also for maize γ-zeins expressed in *Arabidopsis* (Geli *et al.*, 1994), *Nicotiana tabacum* leaves (Bellucci *et al.*, 2000; Mainieri *et al.*, 2004), or *Xenopus* oocytes (Torrent *et al.*, 1994). However, such tandem repeats are lacking in some prolamin sequences such as in rice, indicating that other mechanisms could also be determinants for ER retention. Some studies indicated that the accumulation of prolamins in the ER lumen could simply be the result of the massive aggregation of these proteins, especially due to the insolubility of glutenin compared with gliadin which could initially be soluble in the luminal environment (Rubin *et al.*, 1992; Napier *et al.*, 1997). An ER retention mechanism and formation of PBs based on prolamin interaction with BiP has also been proposed (Levanony *et al.*, 1992; Muench *et al.*, 1997; Saito *et al.*, 2009), but remains to be confirmed, as does the possible interaction of prolamins with membranes to explain their retention in the ER (Geli *et al.*, 1994; Kogan *et al.*, 2004; Vitale and Ceriotti, 2004; Vitale and Hinz, 2005). In the case of wheat, a recent study proposed the involvement of the N-terminal repeated domain of gliadin with model membranes as an anchor for the interaction with the ER (Banc *et al.*, 2009). Also Shimoni and Galili (1996) have shown that disulphide bond formation may play a role in the accumulation of soluble forms of the gliadins in developing wheat grains.

Here the trafficking of wheat γ-gliadin was investigated in order to better understand the mechanisms of its retention in the ER and of PB formation, and to examine the influence of specific molecular characteristics of this protein on these mechanisms. For this purpose, a wheat γ-gliadin and the corresponding N-terminal repeated and C-terminal disulphide bond-rich domains were fused with fluorescent proteins. These fusion proteins were expressed in a heterologus tobacco system in order to avoid any possible effect of wheat endosperm tissue specificity and to study prolamin trafficking specified by their own structural characteristics. The results demonstrated that not only γ-gliadin, but also both its domains fused with fluorescent proteins are retained in the ER and are able to form mobile bodies. Moreover, when stably transformed in BY-2 cells, these fusion proteins are then transported into the vacuole for degradation after being retained in the ER for several days.

Materials and methods

Plant material

Nicotiana tabacum sp. plants used for transient expression were grown in the greenhouse at 21 °C with 14 h light/10 h dark for 5–6 weeks prior to *Agrobacterium* infiltration.

Suspension-cultured tobacco cells (BY-2; *N. tabacum* L., cv Bright Yellow 2) were provided by C. Rechenman (ISV, Gif/Yvette, France) and cultured at 24 °C in the dark in a Murashige and Skoog–MES medium (Duchefa, no. M0254) supplemented with 20 mg l^{-1} KH_2PO_4, 100 mg l^{-1} myo-inositol, 30 g l^{-1} sucrose, 1 mg l^{-1} thiamine, and 0.2 mg l^{-1} 2.4 D, pH 5.8.

Plasmid constructs

The binary Gateway vectors pMDC83 (Curtis *et al.*, 2003) and pK7RWG2 (Karimi *et al.*, 2005) containing a double 35S promoter of cauliflower mosaic virus (CaMV) and the enhanced green fluorescent protein (eGFP) or monomeric red fluorescent protein (mRFP1) coding sequences, respectively, were used to construct C-terminal GFP/mRFP fusions to the full-length γ-gliadin and its domains. Gateway system cloning was used to replace the gateway cassette by gliadin and domain sequences according to the manufacturer's instructions (Invitrogen). The cDNA encoding γ-gliadin was amplified by PCR using the primers AttB1-G5-PS (5′-AAA AAA GCA GGC TTC ATG AAG ACC TTA CTC ATC) and AttB2-G5 (5′-CAA GAA AGC TGG GTC TTG GCC ACC AAT GCC) followed by a second PCR with the primers AttB1 (5′-GGG GAC AAG TTT GTA CAA AAA AGC AGG CT) and AttB2 (5′-GGG GAC CAC TTT GTA CAA GAA AGC TGG GT). To obtain the cDNA corresponding to the N-terminal domain of γ-gliadin, cDNA encoding γ-gliadin was amplified by PCR using the primers AttB1-G5-PS and AttB2-QQQ-G5 (5′-CAA GAA AGC TGG GTC CTG TTG TTG TAG ATA TGG). To obtain the cDNA corresponding to the C-terminal γ-gliadin domain with the signal peptide at its 5′ extremity, cDNA encoding γ-gliadin was amplified by PCR using the primers PS-Gb5C-5′ (5′-ATG AAG ACC TTA CTC ATC CTG ACA ATC TTT GCG GCG GCT CTA ACC ATC GCC ACC GCC ATG AAC CCC TGC AAG AAT TAC CTC) and Gb5-3′ (5′-CCT TGG CCA CCA ATG CC) followed by a second PCR using the primers AttB1-G5-PS and AttB2-G5. Full recombination regions for Gateway cloning were added to the N- and C-terminal domains of γ-gliadin in a final round of PCR using the primers AttB1 (5′-GGG GAC AAG TTT GTA CAA AAA AGC AGG

CT) and AttB2 (5′-GGG GAC CAC TTT GTA CAA GAA AGC TGG GT).

For yeast two-hybrid analysis, the cDNA encoding the γ-gliadin domains was amplified by PCR using the following primers: NcoI-NIQ5′ (5′-C CAT GCC ATG GCA AAT ATA CAG GTC GAC CCT AGC GGC) and BamHI-QQQ3′ (5′-CG GGA TCC TCA TTG TTG TTG CAA AAT TTG TTG AAG) for the N-terminal domain sequence, and NcoI-MNP5′ (5′-C CAT GCC ATG GCA ATG AAC CCC TGC AAG AAT TAC CTC) and BamHI-GGQ3′ (5′-CG GGA TCC TCA TTG GCC ACC AAT GCC GGC) for the C-terminal domain sequence. The PCR products were cloned into pACT2 prey vector (*2μ pADH1Δ GAL4-AD LEU2 Amp^R*) (Clontech) and pAS2-1 bait vector (*2μ pADH1 GAL4-BD TRP1 Amp^R*) (Clontech), using the *Nco*I and *Bam*HI as restriction sites.

Expression of fluorescent protein fusions in tobacco plants

Agrobacterium-mediated infiltration of tobacco leaf epidermal cells was performed as described by Sparkes *et al.* (2006). Briefly, *Agrobacterium tumefaciens* GV3101::mp90 were transformed by heat shock with the binary gateway–plasmid vectors described above. The transformants were inoculated into 4 ml of YEB medium (5 g l^{-1} beef extract, 1 g l^{-1} yeast extract, 5 g l^{-1} peptone, 5 g l^{-1} sucrose, 2 mM MgSO$_4$) supplemented with 10 μg ml^{-1} gentamycin and 50 μg ml^{-1} spectinomycin or 100 μg ml^{-1} kanamycin, and grown at 28 °C overnight. Cells were centrifuged and washed once with infiltration buffer (5 g l^{-1} glucose, 50 mM MES, 2 mM Na$_3$PO$_4$·12H$_2$O, 100 μM acetosyringone) before being resuspended with the same buffer at an optical density (λ=600 nm) of 0.1 and 0.05 for gliadin constructs and marker vectors [Golgi, ER, and pre-vacuolar compartment (PVC)], respectively. Lower leaves of *N. tabacum* sp. plants were infiltrated with the diluted bacteria using a syringe. For co-expression the bacteria were mixed in appropriate volumes of infiltration buffer prior to injection into the leaves. Fluorescent protein expression was studied 2–3 d after infiltration.

Drug treatments

For actin depolymerization, tobacco leaf samples were incubated in a 25 μM solution of latrunculin B (Calbiochem, UK). Drug treatment was performed for 40 min. The working solution of latrunculin B was prepared fresh from a frozen stock solution [1 mM in dimethylsulphoxide (DMSO)].

For brefeldin A (BFA) experiments, BFA (Sigma Aldrich, stock solution at 2.5 mg ml^{-1} in DMSO) was added at 10 μg ml^{-1} to 4-day-old BY-2 suspension cells during 2 h or 5 h. Each drug treatment for confocal imaging was repeated at least twice with similar results.

Stable transformation of BY2 cells

The constructs were transferred into *A. tumefaciens* GV3101::mp90 by heat shock. Transformed *Agrobacterium* were selected in YEB medium containing gentamycin (10 μg ml^{-1}) and spectinomycin (50 μg ml^{-1}) or kanamycin (100 μg ml^{-1}) according to the individual construct, and were used to transform BY-2 cells as previously described (Gomord *et al.*, 1998). Transformed BY-2 cells were selected on solid medium containing kanamycin (100 μg ml^{-1}) or hygromycin (40 μg ml^{-1}), according to the selection gene carried by the construct, and cefotaxim (250 μg ml^{-1}). Then transformed BY-2 calli were screened by fluorescence microscopy and selected calli were used to initiate transgenic suspension cell cultures.

Confocal microscopy

An inverted Zeiss LSM 510 confocal laser scanning microscope (CLSM; Zeiss UK, Welwyn Garden City, UK) equipped with ×40, ×63, and ×100 oil immersion objectives was used to examine the subcellular localization of GFP and mRFP fluorescence. GFP was excited at 488 nm with an argon ion laser and emission was detected using a 488/543 nm dichroic beam splitter and a 505–530 nm bandpass filter. mRFP was excited with a helium ion laser of 543 nm and emission was detected using a 458/543 nm dichroic beam splitter and a 560–615 nm bandpass filter. For imaging GFP in combination with mRFP, excitation lines of an argon ion laser of 488 nm and a helium ion laser of 543 nm were used alternately with line switching, using the multitrack facility of the CLSM.

Electron microscopy

Small squares of γ-gliadin-expressing leaf were fixed for 1 h in 1% glutaraldehyde and 1% paraformaldehyde in sodium cacodylate buffer pH 6.9, and washed in buffer and distilled water. Specimens were then post-fixed in 1% aqueous OsO$_4$ for 1 h, washed in distilled water, and stained overnight in 2% aqueous uranyl acetate at 4 °C. Following sequential dehydration in a water/ethanol series, material was embedded in Spurr resin, polymerized, sectioned with an RMC Powertome XL ultramicrotome, stained with lead citrate, and observed with a Hitachi H7650 transmission electron microscope.

Protein extraction from BY-2 and tobacco leaf epidermal cells

Tobacco BY-2 cells were gently filtered and resuspended in 500 μl of SDS sample buffer (100 mM TRIS-HCl, pH 6.8, 4% SDS, 20% glycerol, 5% 2-mercaptoethanol, 100 μg ml^{-1} bromophenol blue). After boiling for 5 min, the sample was centrifuged for 5 min at 1000 rpm and the supernatant was subjected to SDS–PAGE and then to immunoblotting with specific antibodies. Each extract loaded on the gel corresponded to the same volume of filtered cells.

Infiltrated tobacco leaf sections were cut, crushed in liquid nitrogen, rinsed in acetone, and dried. The leaf powder was weighed and resuspended in SDS sample buffer, boiled, and centrifuged as described above.

Western blot analysis

Immunoblotting was performed using protein extracts from transformed cultured cells or infiltrated leaves. A wheat seed gliadin extract and a recombinant yellow fluorescent protein (YFP) extract produced in *Escherichia coli* were used as positive controls. After SDS–PAGE analysis, separated proteins were electrotransferred to a nitrocellulose membrane (Invitrogen), revealed using mouse monoclonal anti-GFP antibodies (dilution 1:2500) (Clontech), and detected with an alkaline phosphatase-conjugated goat anti-mouse antibody (dilution 1:2000). Proteins were stained with 5 bromo-4-chloro-3-indoyl phosphate (BCIP) and nitroblue tetrazolium (NBT) (Kit Promega) according to the manufacturer's instructions.

Yeast two-hybrid assay

Yeast two-hybrid analysis was performed in *Saccharomyces cerevisiae* strain Y190 [*MATa, gal4, gal80, his3, trp1, ade2, ura3, leu2, URA3::GAL1::lacZ, LYS2::GAL4(UAS)::HIS3 cyh^R*]. Y190 was transformed by a pair of plasmids expressing Gal4-BD-fusion *TRP1* (bait)/Gal4-AD-fusion *LEU2* (prey) and plated onto selective media for up to a period of 5 d at 30 °C. Positive yeast transformants were replated and tested for β-galactosidase production in an overlay plate assay.

FRET-FLIM assay

The C-terminal γ-gliadin domain fused to GFP was expressed by itself and in combination with the N-terminal γ-gliadin domain fused to mRFP in tobacco leaf epidermal cells. Three days after infiltration leaf pieces were excised and incubated in latrunculin B (25 μM) for 30–60 min. Expression and FRET-FLIM analysis was

carried out according to Sparkes *et al.* (2010) except that lifetimes of individual pixels rather than regions of interest were measured and quantified.

Results

Construction of gliadin fluorescent fusions

To investigate the trafficking of wheat gliadin and to better understand the mechanisms involved in its trafficking, C-terminal mRFP/GFP fusions of full-length γ-gliadin or its repeated N-terminal domain and disulphide bond-rich C-terminal domain were generated. All these constructs contained the signal peptide of γ-gliadin at the N-terminal extremity of the sequences (Fig. 1). As the expression level of the prolamins is very high in wheat seed endosperm cells, the gliadin sequences were put under the control of the double CaMV 35S promoter which allows strong expression of proteins. The GFP or mRFP constructs were transiently expressed in tobacco leaves via *Agrobacterium* infiltration or stably expressed in a BY-2 tobacco cell line, and the subcellular localization was analysed by confocal laser scanning microscopy.

Subcellular localization of the full-length γ-gliadin in transiently transformed tobacco leaf epidermal cells

First the subcellular localization of full-length γ-gliadin was examined in order to determine whether tobacco cells are an appropriate model to study wheat prolamin trafficking. For this purpose, transient expression of γ-gliadin–GFP was monitored in *Agrobacterium*-infiltrated tobacco leaves. γ-Gliadin–GFP fluorescence was detected in the ER of tobacco cells 2–3 d after infiltration (Fig. 2A). The same pattern was observed with the γ-gliadin fused to mRFP (Fig. 2B). Co-localization of γ-gliadin–GFP with an ER marker (mRFP$_1$–DPL1; Marion *et al.*, 2008) confirmed that the wheat prolamin is present in this compartment (Fig. 2C). In addition, full-length γ-gliadin also formed numerous punctate structures. These were present at
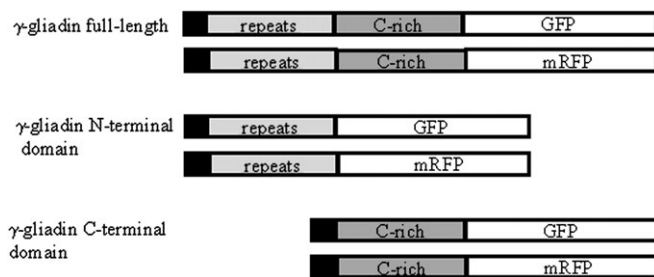

Fig. 1. Schematic representation of the γ-gliadin constructs used in the study. All fusion constructs were placed under the control of the cauliflower mosaic virus double 35S promoter and the nopaline synthase terminator. Repeats, N-terminal repeated sequence of γ-gliadin; C-rich, C-terminal cysteine-rich sequence of γ-gliadin; GFP, green fluorescent protein; mRFP, monomeric red fluorescent protein; black square, γ-gliadin ER signal peptide. The diagram is not drawn to scale.

various sizes, from <1 μm to >5 μm in diameter, and co-localized with the ER marker or were surrounded by ER in the case of larger bodies. Similar structures surrounded by membrane were also described in leaf cells when a rice prolamin GFP fusion was expressed in transgenic rice (Saito *et al.*, 2009). This result indicates that wheat γ-gliadin is retained in the ER where it forms protein body-like structures (PBLS). The sizes of the observed PBs are consistent with those found in wheat endosperm cells during the early stages of development (Loussert *et al.*, 2008).

Electron microscopy of γ-gliadin-expressing leaf epidermal cells exhibited dilated profiles of tubular ER reflecting the punctate structures seen by confocal microscopy (Fig. 2F). In other areas of the cytoplasm rough ER showed more normal profiles (Fig. 2G).

It is known that GFP fused to a vacuolar target is often undetectable in the vacuole under light-grown conditions, and fluorescence is only detectable when the plants are kept in the dark (Tamura *et al.*, 2003). To check the possibility that γ-gliadin–GFP could be transported to the vacuole, infiltrated tobacco plants were put in the dark 24 h after infiltration, and the subcellular localization of the γ-gliadin–GFP was observed with confocal microscopy 1 d and 2 d later. No fluorescence was noted in the vacuole in such plants (data not shown) and the subcellular localization of γ-gliadin–GFP was exactly the same as in the light-grown plants.

Movement of γ-gliadin protein body-like structures is highly dynamic and actin dependent

It was observed in the present experiments that γ-gliadin PBLS were highly mobile, as shown by time-lapse confocal images of the fluorescent PBLS expressed in the leaf epidermal cells (Fig. 3; see Supplementary Movie S1 available at *JXB* online). The PBLS exhibited various patterns of movement. Generally PBLS follow no continuous directional movement. While some PBLS appeared to follow a directional movement for some time, these same PBLS could then move in a stop and go manner, or seemed to be relatively static at other times. The images demonstrate that PBLS moved throughout the cell along the ER network. While the significance of the movement of these PBLS is not clear, it is suggested that movements could allow fusion or coalescence of PBLS, thus explaining the range of sizes of PBLS and why these larger PBLS were more often observed 4 d after infiltration. Thus, there was a possible correlation between PBLS size, movement, and duration of expression. To examine the actin dependence of γ-gliadin PBLS movements, transformed leaf material was incubated with latrunculin B to disrupt actin filament organization. After 40 min of treatment, no movement of PBLS was observed, indicating that γ-gliadin PBLS mobility is actin dependent.

γ-Gliadin–GFP PBLS are very mobile and their movement pattern is similar to, and their sizes are in the same range as, the motile Golgi bodies. For this reason, it was decided to co-express the γ-gliadin–GFP with a Golgi marker [the rat sialyl transferase signal anchor sequence
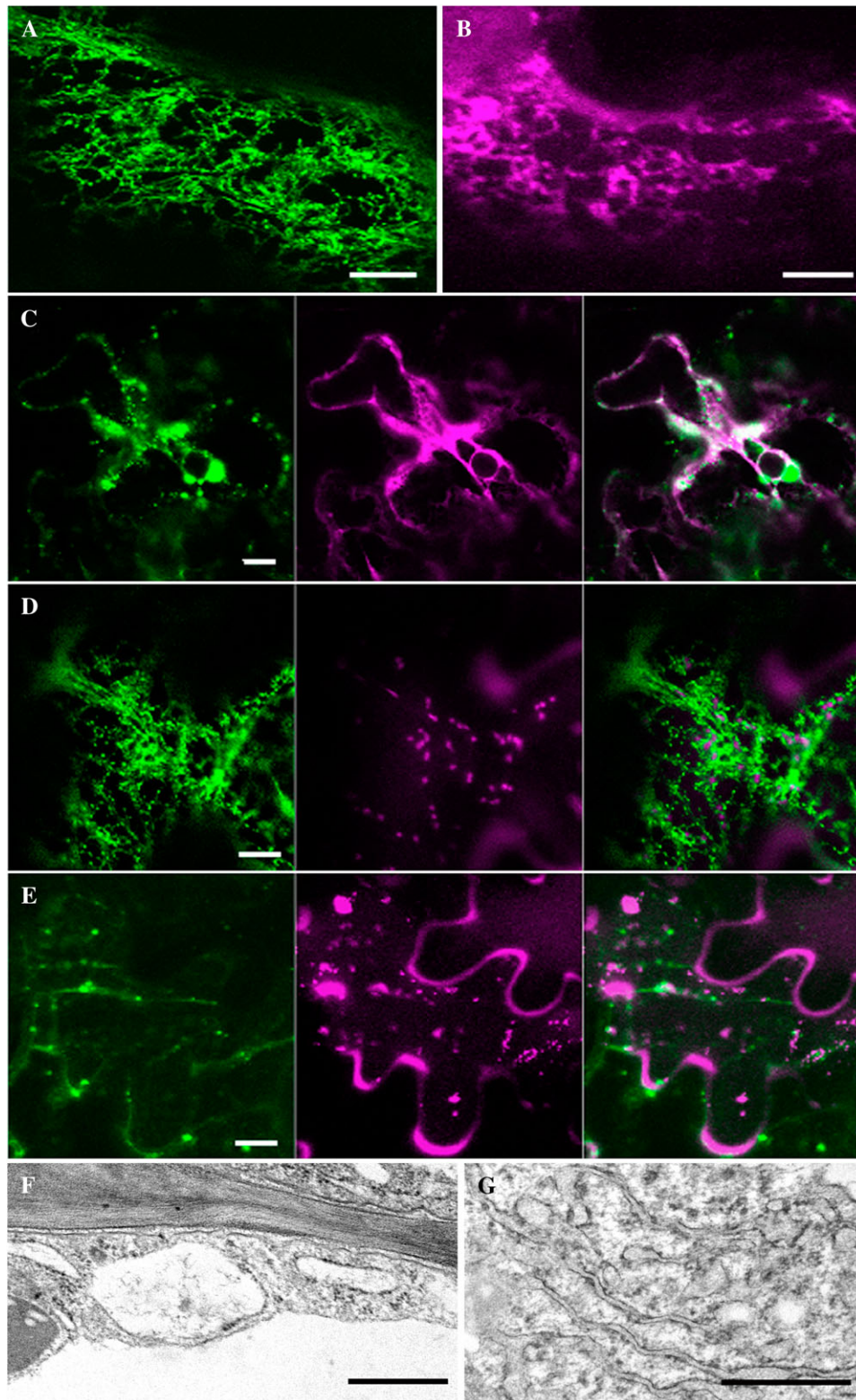
Fig. 2. The subcellular localization of full-length γ-gliadin fluorescent fusions in tobacco epidermal cells. Confocal and electron microscope images showing GFP (green) and mRFP (magenta) fusion proteins co-expressed in tobacco leaf epidermal cells 2–3 d after infiltration with *Agrobacterium* suspension cultures. Images of cells expressing (A) γ-gliadin–GFP, (B) γ-gliadin-mRFP, (C) γ-gliadin–GFP (green) co-expressed with an mRFP$_1$-DPL1 ER marker (magenta), and merged image, (D) γ-gliadin–GFP (green) co-expressed with a Golgi marker, ST–mRFP (magenta), and merged image, (E) a PVC marker, RabF2b–GFP (green) co-expressed with γ-gliadin–mRFP (magenta), and merged image. Electron micrographs show areas in leaf epidermal cells expressing γ-gliadin–GFP where the ER is dilated (F) and areas where the rough ER demonstrates conventional profiles (G). A–E scale bars=10 μm. F, G scale bars=500 nm.
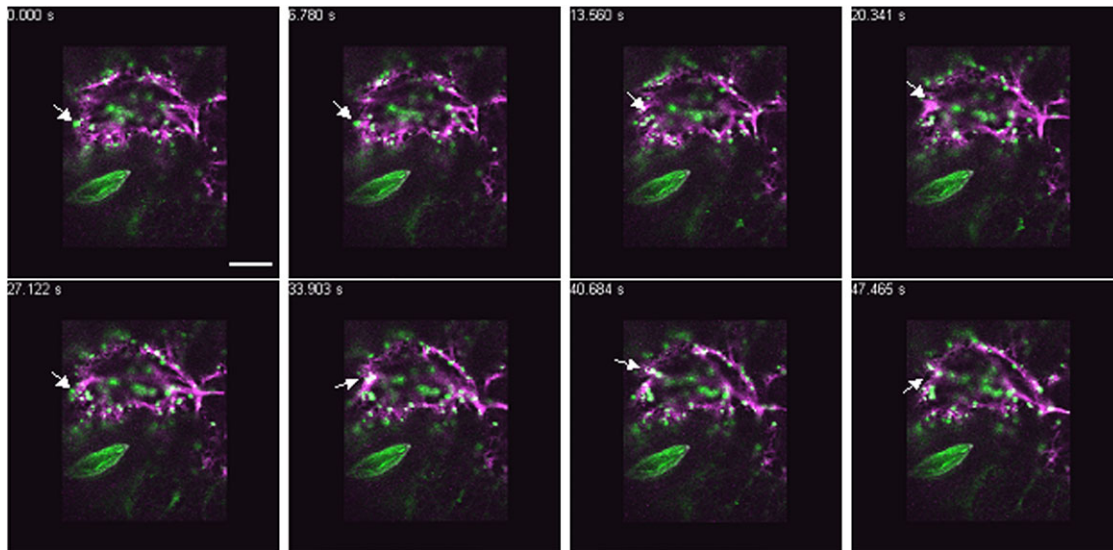
Fig. 3. Tracking γ-gliadin protein body-like structure movement. Time-lapse series of confocal images taken over 47.465 s showing γ-gliadin–GFP infiltrated at OD_{600}=0.1 (green) and the $mRFP_1$–DPL1 ER marker at OD_{600}=0.05 (magenta) in tobacco epidermal leaf cells. Arrowheads indicate the movement of a γ-gliadin–GFP protein body-like structure over the ER surface. Scale bar=10 μm.

(ST) fused to mRFP] which traffics from the ER to the Golgi. The result indicates that γ-gliadin PBLS do not appear to co-localize with Golgi bodies (Fig. 2D; see Supplementary Movie S2 at *JXB* online).

A RabF2b protein fusion was also co-expressed to confirm that the PBLS did not co-localize with post-Golgi compartments such as the PVC. RabF2b is involved in the endocytic pathway, and is also required for the sorting of a vacuolar marker to the central vacuole of tobacco leaf epidermal cells via the PVC, most probably by cycling between the Golgi and PVC compartments (Kotzer *et al.*, 2004). Here it is shown that γ-gliadin PBLS do not localize with the PVC (Fig. 2E).

These results indicate that γ-gliadin PBLS synthesized and retained in the ER do not co-localize with Golgi bodies or PVCs, and move along the ER network. In addition, there was a possible correlation between PBLS size, movement, and duration of expression. This suggested that a similar trafficking pathway occurs for artificially expressed prolamins in tobacco cells compared with native expression in wheat endosperm cells during the early stages of development. Therefore, this particular pathway would not be due to the specific seed tissue, but more probably due to the specific gliadin sequence.

Both domains of γ-gliadin are retained in the ER and form protein body-like structures

γ-Gliadin possesses two distinct domains that appear to fold independently of each other (Tatham *et al.*, 1990): a hydrophilic glutamine- and proline-rich repetitive N-terminal domain, and a disulphide bond-rich C-terminal domain. To determine the important elements of the protein necessary for retention in the ER and formation of PBs, fusions of these two distinct domains with fluorescent proteins under the control of a double 35S promoter were constructed (Fig. 1). For both constructs the endogenous signal peptide of γ-gliadin was added at the N-terminal extremity for insertion into the ER. These two truncated γ-gliadin constructs were then used to transiently transform tobacco leaves. Expression of the separate domains of γ-gliadin indicated that both of them were retained in the ER and formed PBLS (Fig. 4A, B), as confirmed by co-expression with an ER marker (Fig. 4C, G). Immunoblot analysis with anti-GFP antibodies revealed the stability of all three fusions (the full-length protein, and the N-and C-terminal domains fused to GFP; Fig. 5A). While it was expected that the N-terminal domain would be seen in the ER as reported previously when expressed in *Xenopus* oocytes or yeast (Altschuler *et al.*, 1993; Rosenberg *et al.*, 1993, respectively), the retention of the C-terminal domain in the ER was more surprising. Nevertheless the C-terminal domain formed fewer and smaller PBLS than the N-terminal domain (Table 1), and seems also to be partly present in the cytoplasm, indicating that this domain is perhaps less stable than the other. This hypothesis was highlighted by the fact that a fragment of lower mobility corresponding to the mass of free GFP was detected in the C-terminal γ-gliadin–GFP sample (Fig. 5A). Also quantitative data indicated a lower level of accumulation of the C-terminal domain compared with that of full-length and N-terminal γ-gliadin (Fig. 5B). Also it was not possible to express this C-terminal domain correctly when fused with mRFP, the corresponding fusion protein being unstable. The absence of transport to the vacuole was again confirmed in dark-incubated plants. These PBLS are also mobile like the PBLS formed with full-length γ-gliadin (see Supplementary Movies S3, S4 at *JXB* online), and latrunculin treatment showed that the mobility of these PBLS was also actin dependent (not shown). These PBLS are similar in size to those observed with the full-length
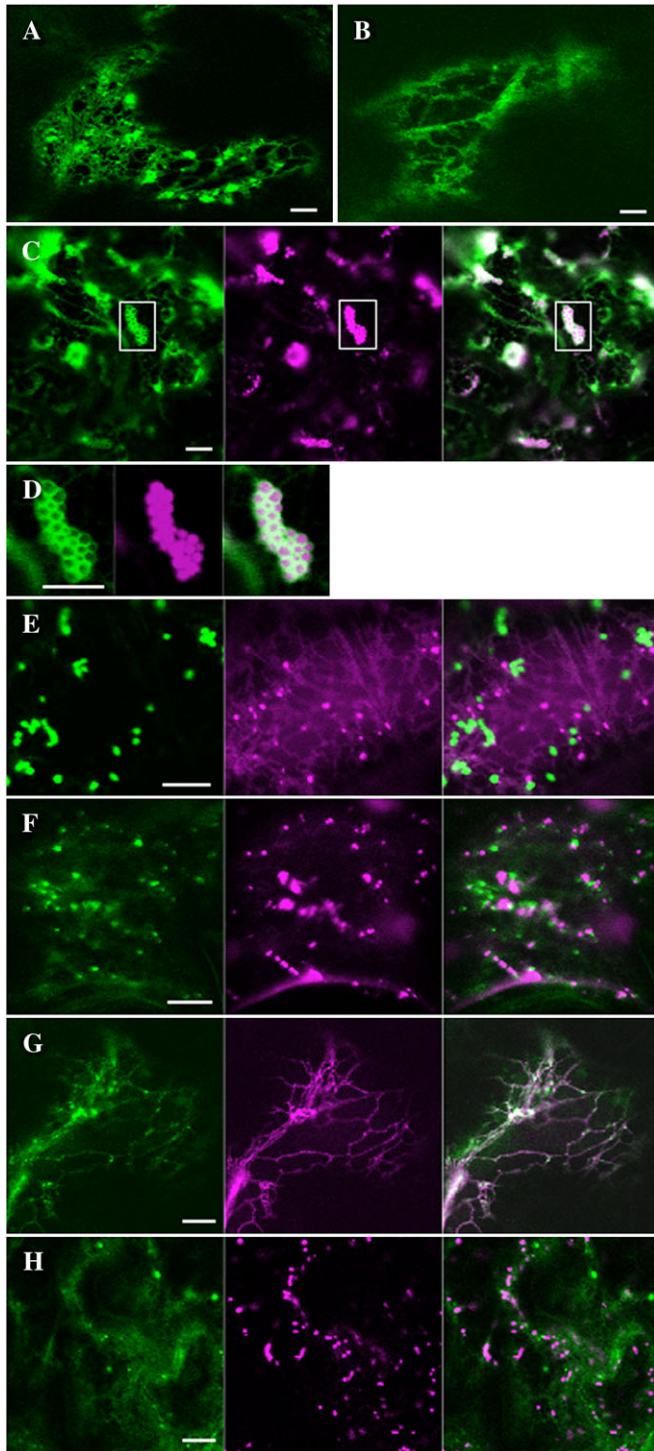
Fig. 4. The subcellular localization of the N- and C-terminal domains of γ-gliadin fused to fluorescent protein in tobacco epidermal cells. Confocal images showing GFP (green) and mRFP (magenta) fusion proteins co-expressed in tobacco leaf epidermal cells 2–3 d after *Agrobacterium* infiltration. Images of cells expressing (A) Nter-γ-gliadin–GFP, (B) Cter-γ-gliadin–GFP, (C) co-expression of Nter-γ-gliadin–mRFP (magenta) with the GFP–DPL1 ER marker (green) (a higher magnification of the inset in C is shown in D), (E) the ST–GFP Golgi marker (green), (F) the RabF2b–GFP pre-vacuolar compartment marker (green), (G) co-expression of Cter-γ-gliadin–GFP (green) with the mRFP$_1$–DPL1 ER marker (magenta), or (H) the ST–mRFP Golgi marker (magenta). Scale bars=10 μm.

γ-gliadin, and the N-terminal domain fusion was frequently observed in large PBLS (>5 μm in diameter). With N-terminal γ-gliadin expression, clusters of PBLS resembling bunches of grapes were also observed (Fig. 4C, D). These clusters were surrounded by the ER lumenal marker, therefore indicating that the ER membrane encapsulates the PBLS. This observation tends to confirm that PBLS could gather together as a first step in the process of forming larger bodies by fusion or coalescence. As previously shown with the full-length protein, PBLS formed by the isolated γ-gliadin domains are mobile and they did not significantly co-localize with Golgi bodies (Fig. 4E, H). Moreover, it was demonstrated that the N-terminal domain did not co-localize with a PVC marker (Fig. 4F).

γ-Gliadin domains are present in the same protein body-like structures when co-expressed

When both γ-gliadin domains were co-expressed in tobacco leaf epidermal cells, there was a co-localization of the repetitive N-terminal and the cysteine-rich C-terminal domains in the PBLS (Fig. 6A). All PBLS formed inside the tobacco cells contained both domain fusions. As seen previously, the C-terminal domain was also partly observed in the cytoplasm. Moreover at the resolution offered by confocal microscopy these domains appeared homogeneously distributed inside PBLS. This result led to the investigation of the possibility that the γ-gliadin domains could interact with each other. Interaction between the N- and C-terminal domains of γ-gliadin was therefore analysed *in vitro* using the yeast two-hybrid system. Both domains were fused at their N-termini with the activation domain or the binding domain of the yeast transcription factor GAL4 to test both interaction possibilities. Prey and bait were co-transformed into yeast and the transformants plated onto selection medium. Both combinations, GAL4AD-Nter γ-gliadin/GAL4BD-Cter γ-gliadin and GAL4AD-Cter γ-gliadin/GAL4BD-Nter γ-gliadin, produced positive colonies for β-galactosidase activity, indicating that the two domains of γ-gliadin interact in yeast (Fig. 6B). Negative controls indicated that both domains are not able to interact directly with the activator domain or the binding domain of the GAL4 transcription factor.

To assess the interaction *in planta*, FRET-FLIM analysis was undertaken. Tobacco leaf epidermal cells expressing either C-terminal γ-gliadin fused to GFP or in combination with N-terminal γ-gliadin fused to mRFP were excised and the interaction was tested. The fluorescence lifetime of C-terminal γ-gliadin fused to GFP in cells co-expressing both N- and C-terminal γ-gliadin fusions was significantly reduced compared with cells only expressing C-terminal γ-gliadin–GFP [Fig. 6C; 1.70 ± 0.12 ns (mean $\pm$SD) compared with 2.19 ± 0.1 ns (mean $\pm$SD), respectively, $P < 0.001$ *t*-test]. The significant reduction of >0.1 ns indicates that in plants the N- and C-terminal domains of γ-gliadin interact, confirming the yeast two-hybrid studies.
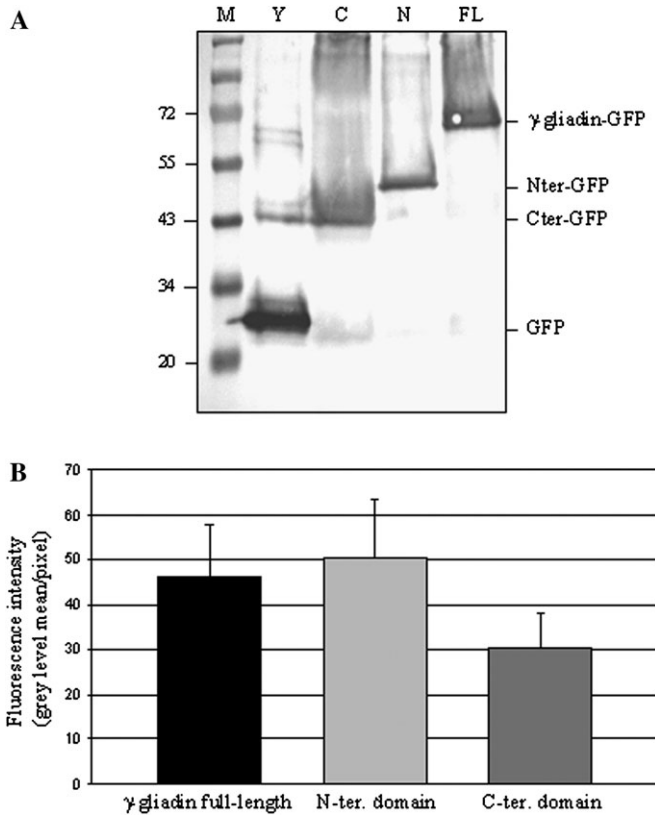
A

B

Fig. 5. Immunoblotting and fluorescence intensity quantification from tobacco leaf epidermal cells expressing γ-gliadin or its domains. (A) An immunoblot was performed with anti-GFP antibodies. M, protein marker; Y, tobacco leaf infiltrated with a YFP construct as a positive control; C, tobacco leaf expressing C-terminal γ-gliadin–GFP; N, tobacco leaf expressing N-terminal γ-gliadin–GFP; FL, tobacco leaf expressing full-length γ-gliadin–GFP. (B) Fluorescence intensity quantification from tobacco leaves expressing the fusion proteins. Fluorescence intensities were measured from confocal images of tobacco leaves expressing full-length γ-gliadin–GFP, Nter-γ-gliadin–GFP, or Cter-γ-gliadin–GFP proteins. They are expressed as the grey level mean per pixel.

Gliadin–GFP is retained in the ER and then transported and degraded in the vacuole during the growth of BY-2 cells

Full-length γ-gliadin and its domains were expressed in a stable expression system to examine the long-term trafficking of γ-gliadin in tobacco cells. BY-2 culture cells were transformed with γ-gliadin–GFP, Nter γ-gliadin–GFP, or Cter γ-gliadin–GFP. Confocal laser scanning microscopy clearly showed that fluorescence was observed in the ER for the full-length γ-gliadin–GFP and for both the N- and C-terminal domains of gliadin fused to GFP when cells from stable transgenic lines were examined a few days after subculturing (2–3 d) (Fig. 7A, C, E). This is in accordance with the observations made in transiently transformed tobacco leaves reported above. Some punctate structures were also observed when the full length γ-gliadin and its domains fused to GFP were expressed in BY-2 cells, but these structures were generally smaller and less numerous than in the tobacco leaf system (Table 1). In addition, as seen in infiltrated tobacco leaf epidermal cells, stable expression in BY-2 cells showed a lower expression level of Cter γ-gliadin–GFP compared with that observed with full-length γ-gliadin–GFP and Nter γ-gliadin–GFP (Fig. 7G). When cells were observed 4–6 d after subculturing, that is after the exponential cell growth phase, the fluorescence appeared not only in the ER but also in the vacuole (Fig. 7B, D, F). With age the intensity of the fluorescence in the vacuole increased, suggesting that γ-gliadin–GFP is transported into the vacuole after being retained for several days in the ER. Such observations were previously reported for other ER-resident proteins such as BiP and PDI which were shown to be constitutively transported to the vacuole for degradation (Tamura *et al.*, 2004). Moreover, analysis of fusion protein expression by immunoblotting with an anti-GFP antibody indicated that 4 d after subculturing, protein expression corresponded mainly to γ-gliadin–GFP (58 kDa) with a small component of free GFP at 27 kDa. Detection of γ-gliadin–GFP progressively decreased with time in culture, and at 10 d after subculturing

Table 1. Classification of the transformed cells containing protein body-like structures

Cells were provided from at least three individual transformation experiments in tobacco leaf cells or BY-2 cells, transformed with each of the three constructs. The values are expressed as a percentage. Analysed cells were classified into three categories according to the density of gliadin puncta within the ER [corresponding to protein body-like structures (PBLS)]. The analysis was generated from confocal sections of transformed cells. The first category corresponds to cells containing no apparent gliadin puncta; the second category corresponds to cells containing a low PBLS density (<5 puncta 10 μm^2); and the third category corresponds to cells containing a high PBLS density (>5 puncta 10 μm^2). The size of PBLS was taken into account in classification of cells.

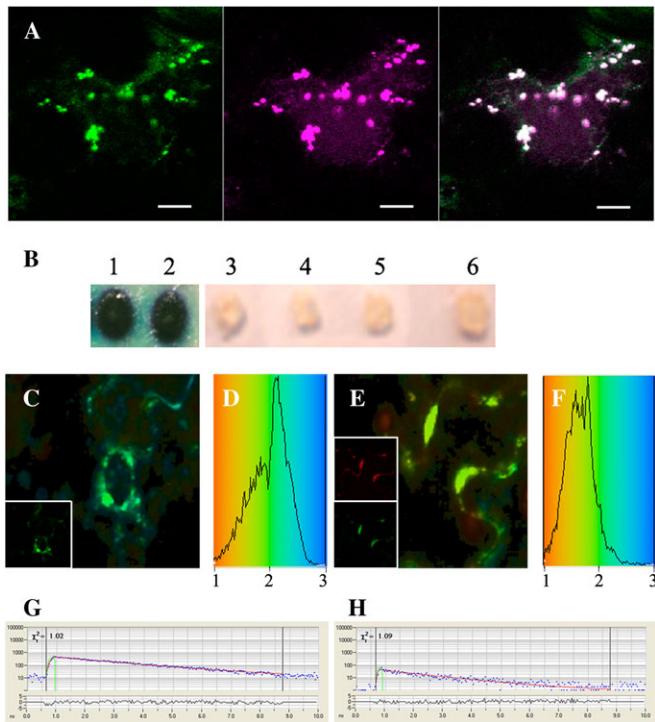|		Without apparent ER puncta	Low ER puncta density		High ER puncta density	
			Puncta <1 μm	Puncta >1 μm	Puncta <1 μm	Puncta >1 μm
Leaves of tobacco cells	Full length–GFP	1	9.5	17.9	31.6	**40**
	N-ter–GFP	2.4	8.3	17.8	26.3	**45.2**
	C-ter–GFP	12.9	**54.9**	16.1	11.3	4.8
BY-2 cells (<4 d of culture)	Full length–GFP	9.6	22.3	24.2	**27.7**	16.2
	N-ter–GFP	6.3	**28.4**	25.3	24.7	15.3
	C-ter–GFP	16.3	**55.8**	9.3	13.9	4.7

Fig. 6. N- and C-terminal domains of γ-gliadin fused to a fluorescent protein locate to the same protein body-like structures in tobacco leaf epidermal cells and interact in yeast two-hybrid assays and *in planta*. (A) Confocal images of tobacco leaf epidermal cells transiently expressing Cter-γ-gliadin–GFP (green) and Nter-γ-gliadin–mRFP (magenta). Constructs were infiltrated and imaged 3 d after inoculation. (B) The interaction of N- and C-terminal domains of γ-gliadin was studied using the yeast two-hybrid system where: (1) pACT-Nter-γ-gliadin+pAS-Cter-γ-gliadin; (2) pACT-Cter-γ-gliadin+pAS-Nter-γ-gliadin; (3–6) negative controls; (3) pACT-Nter-γ-gliadin+empty pAS vector; (4) pACT-Cter-γ-gliadin+empty pAS vector; (5) empty pACT vector+pAS-Nter-γ-gliadin; (6) empty pACT vector+pAS-Cter-γ-gliadin. A representative patch is shown. (C–H) FRET-FLIM analysis in tobacco leaf epidermal cells. Lifetime images of Cter-γ-gliadin–GFP (C) and Cter-γ-gliadin–GFP in a cell co-expressing Nter-γ-gliadin–mRFP (E) are shown. Insets are confocal images showing expression of Nter-γ-gliadin–mRFP (red) and/or Cter-γ-gliadin–GFP (green) in the cells shown. Cter-γ-gliadin–GFP lifetimes were randomly selected within the protein body-like structures within the cell where the lifetime decay curves had χ^2 values between 0.9 and 1.4 (G–H). The lifetime values are shown in D and F and pseudocoloured accordingly in C and E. The lifetime of the combination is >0.1 ns lower than that of the donor fusion, Cter-γ-gliadin–GFP, alone, indicating interaction between Nter- and Cter-γ-gliadin.

there was only free GFP as shown by immunoblotting (Fig. 7H). Taken together with the fact that at 10 d fluorescence was observed only in the vacuole by confocal microscopy, it was concluded that such fluorescence corresponded to GFP alone. In addition, an immunoblotting experiment performed with cells expressing γ-gliadin–GFP submitted to differential centrifugation showed that free GFP was found in the supernatant fraction (corresponding to the soluble vacuolar fraction) whereas gliadin–GFP was mainly found in the pellet fraction (Fig. 7I). This result confirmed that vacuolar fluorescence corresponded to free GFP and that gliadin–GFP accumulated in the ER. Thus γ-gliadin–GFP seems to be transported to the vacuole, and then degraded, leaving free GFP. This is consistent with the fact that GFP–HDEL expressed in BY-2 cells is transported from the ER to the vacuoles and then trimmed into GFP after several days of culture in a manner similar to ER-resident proteins (Tamura *et al.*, 2004). The fluorescence intensity found in the vacuoles of BY-2 cells expressing γ-gliadin–GFP did not decrease during the stationary phase and even increased until 10 d of subculturing, as observed by confocal microscopy and visualized with immunoblotting, suggesting a low turnover of the protein. To establish whether vacuolar delivery was a Golgi-mediated event, treatment with BFA was performed (Fig. 8A). The results indicated that BFA seemed to prevent gliadin–GFP from escaping the ER. After 2 h of treatment there was some residual vacuolar fluorescence, which could be residual GFP left in the vacuoles. After 5 h of BFA treatment, fluorescence was only localized as aggregates in the ER. In addition, the results show that over time these aggregates become larger. Analysis of gliadin–GFP expression with an anti-GFP antibody indicated that after 5 h of BFA treatment there was a reduced pool of free GFP indicative of a reduced amount of degraded gliadin–GFP in the vacuole (Fig. 8B).

The accumulation of the fluorescence in the vacuole during the stationary phase was also observed with the N- and C-terminal γ-gliadin domains fused to GFP, and the 27 kDa GFP was detected when corresponding transformed cells were subjected to an immunoblot with an anti-GFP antibody (data not shown).

Discussion

Currently there are few reports on the expression of fluorescent prolamin fusions (Foresti *et al.*, 2008; Saito *et al.*, 2009), whereas the reliable and common use of GFP cargo protein has been widely applied to study sorting in the plant secretory pathway. To the authors' knowledge, this is the first reported example of a fluorescent protein fusion with a wheat prolamin and demonstrates the power of the technique to study wheat gliadin trafficking. Fusions of gliadin with GFP or mRFP in the tobacco leaf model were retained in the ER which is the same as occurs for endogenously expressed prolamins in wheat endosperm cells (Levanony *et al.*, 1992; Shewry *et al.*, 1995).

Full-length γ-gliadin and also the N- and C-terminal domains of γ-gliadin fused to fluorescent proteins are able to form PBLS that accumulate fused proteins, and regions of dilated ER were observed by electron microscopy. These ER-derived structures in tobacco leaf epidermal cells are sometimes irregular in shape and lack the typical electron-opaque core, which differentiates them from the 'classical' PBs found in wheat endosperm. The PBLS formed in
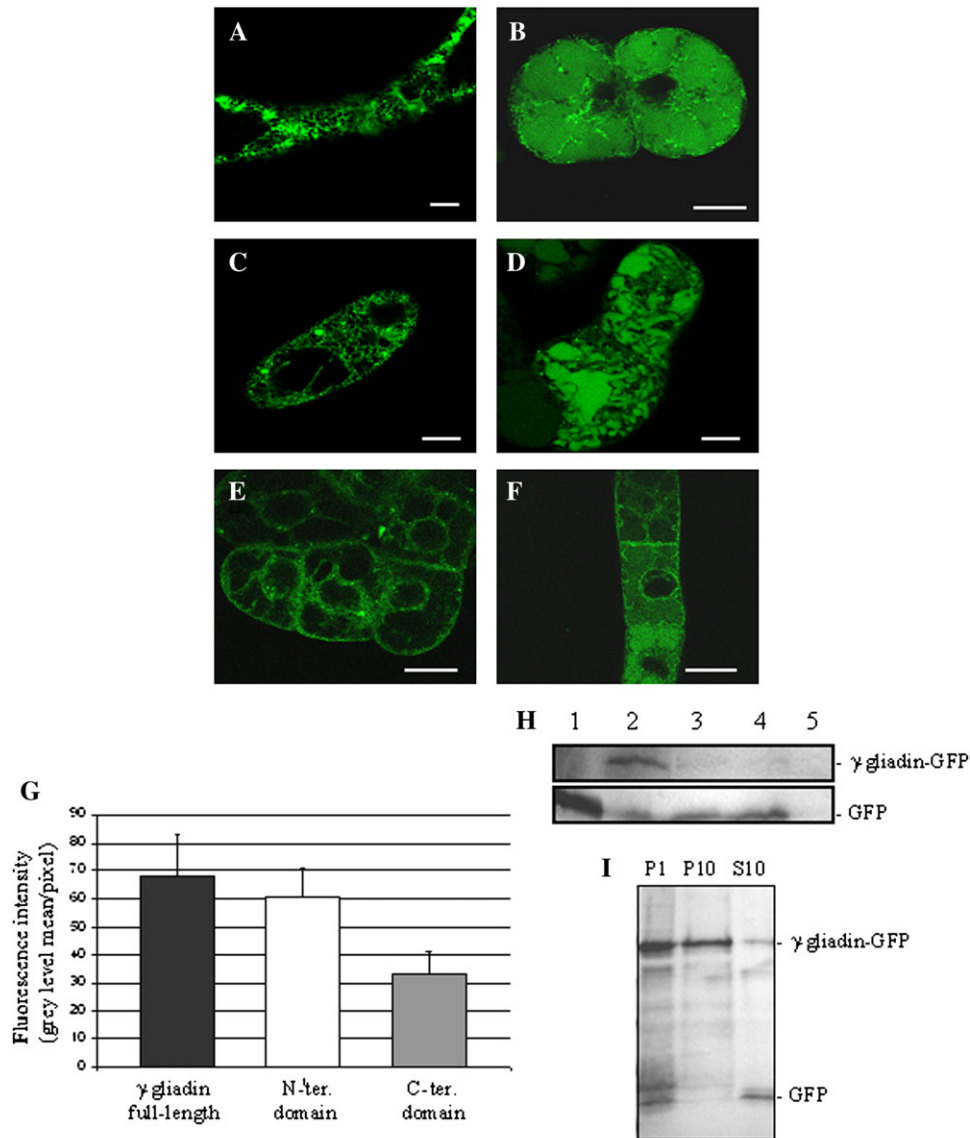
Fig. 7. The subcellular localization of γ-gliadin and domain fusions to GFP in stable transgenic BY-2 cells. (A and B) Subcellular localization of full-length γ-gliadin–GFP expressed in BY-2 cells 3 d (A) or 6 d (B) after subculturing. (C and D) Subcellular localization of N-ter-γ-gliadin–GFP expressed in BY-2 cells 3 d (C) or 6 d (D) after subculturing. (E and F) Subcellular localization of Cter-γ-gliadin–GFP expressed in BY-2 cells 3 d (E) or 6 d (F) after subculturing. Scale bars=20 μm. (G) Fluorescence intensity quantification from BY-2 cells expressing the fusion proteins. Fluorescence intensities were measured from confocal images of BY-2 cells expressing full-length γ-gliadin–GFP, Nter-γ-gliadin–GFP, or Cter-γ-gliadin–GFP proteins. They are expressed as the mean grey level per pixel. (H) An immunoblot was performed with anti-GFP antibodies. (1) Protein extract of YFP expressed in *E. coli* as a positive control; (2) 4-day-old BY-2 cells expressing γ-gliadin–GFP; (3) 6-day-old BY-2 cells expressing γ-gliadin–GFP; (4) 10-day-old BY-2 cells expressing γ-gliadin–GFP; (5) non-transformed BY-2 cells as a negative control. (I) Immunoblotting performed with an anti-GFP antibody from 4-day-old BY-2 cells expressing γ-gliadin–GFP homogenate subjected to differential centrifugation as previously described (Tamura *et al.*, 2004). P1, pellet fraction after a 1000 *g* centrifugation of the homogenate; P10, pellet fraction after a 10 000 *g* centrifugation of the S1 supernatant; S10, 10 000 *g* supernatant.

tobacco cells are motile in the cytoplasm and dependent on the actin cytoskeleton. Recently, the mobility of PBs formed from the expression of elastin-like polypeptides fused to GFP has been reported in epidermal cells of *Nicotiana benthamiana* (Conley *et al.*, 2009). These bodies were also reported to be motile and dependent on the actin–myosin system. The dynamic nature of the plant ER has recently been discussed (Sparkes *et al.*, 2009*a*), and it is well known

that PBs in the *Arabidopsis* ER are extremely motile (Sparkes *et al.*, 2009*b*). As the gliadin PBLS reported here are in the lumen of the ER it could be that their movement also reflects the natural movement of the whole ER network rather than a specific link to the actin cytoskeleton. PBs are natural ER-derived structures that stably accumulate large amounts of storage proteins in seeds; the mechanisms allowing PB formation and the possibility of producing and
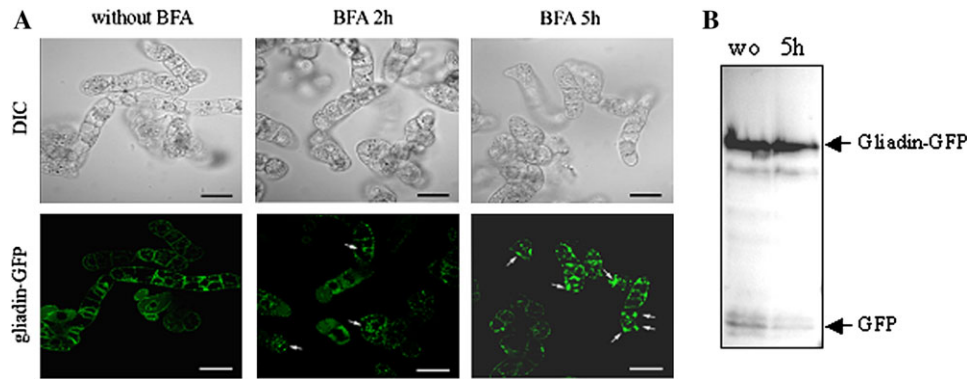
Fig. 8. BFA prevents gliadin–GFP from escaping the ER and induces larger protein body-like structures. (A) Differential interference contrast and fluorescence confocal images of transgenic BY-2 cells expressing full-length γ-gliadin–GFP undergoing BFA treatment. Cells were incubated with BFA at 10 μg ml^{-1} for 2 h or 5 h. Arrows indicate BFA-induced aggregates in cells expressing γ-gliadin–GFP. Scale bars=50μm. (B) Immunoblotting performed with an anti-GFP antibody from BY-2 cells expressing full-length γ-gliadin–GFP, without treatment (wo) or after 5 h of BFA treatment (5h).

accumulating foreign proteins by the same mechanisms were recently reported (De Virgilio *et al.*, 2008; Conley *et al.*, 2009; Torrent *et al.*, 2009). Here it is shown that dynamic PBLS could gather in dense clusters by an actin-related process, which could explain why some PBLS are larger than others in infiltrated tobacco leaves. However, it remains to be determined exactly by which mechanism PBLS are able to gather together and to fuse. This could be related to those observed in the endosperm cells, where an enlargement of prolamin PBs corresponds to the development stage of seeds (Loussert *et al.*, 2008).

It was demonstrated by confocal microscopy that not only full-length and N-terminal repeated domain γ-gliadin were retained and accumulated in the ER, but the C-terminal cysteine-rich domain was also able to be partially retained in the ER and to form PBLS. It seems, however, that the accumulation of the C-terminal domain was less efficient than that observed with full-length γ-gliadin and its N-terminal domain, and this was probably due to fusion protein instability. It has already been shown in heterologous systems that the repeated domain of γ-gliadin was able to be retained and form PBLS (Altschuler *et al.*, 1993; Rosenberg *et al.*, 1993). The repeated domain of maize γ-zein was also able to be retained in the ER but failed to form PBLS without its C-terminal cysteine-rich domain (Geli *et al.*, 1994; Torrent *et al.*, 1994; Mainieri *et al.*, 2004; Pompa et Vitale, 2006). On the other hand, the C-terminal domain localization of wheat γ-gliadin has not been fully studied and this domain was only found to be secreted when expressed in *Xenopus* oocytes (Altschuler *et al.*, 1993). Here it is reported that the C-terminal domain is mainly retained in the ER and forms PBLS in tobacco leaf epidermal cells and BY-2 cells, confirming that the repeated sequence is not the only element responsible for γ-gliadin accumulation.

The fact that both domains of γ-gliadin are able to be retained and form PBs derived from the ER suggests a common explanation for the retention mechanism and/or PBLS formation that would not involve unique structural features of each domain. In the present model system,

γ-gliadin and its N- and C-terminal domains were expressed under the control of the double 35S promoter, which led to strong expression. The overexpression of these proteins could partly explain their accumulation and aggregation in the ER and formation of PBLS, as seen with other foreign overexpressed proteins (Maruyama *et al.*, 2008; Conley *et al.*, 2009). Thus the lower expression level observed with the C-terminal construct could explain its less efficient accumulation in PBLS. In order to investigate the role of protein overexpression further, the involvement of BiP could be examined, as its expression is generally increased during protein aggregation processes and stress events (Vitale and Ceriotti, 2004). In the case of wheat, prolamins are also highly expressed and accumulate in endosperm cells; therefore, overexpression of gliadin in the tobacco system used here is a good way to get closer to the native expression of prolamins. If overexpression is the explanation for the ER accumulation of gliadin in tobacco leaf cells or BY-2 cells, it could be the same in wheat seeds. Napier *et al.* (1997) showed that wild-type γ-gliadin expressed in transgenic tobacco plants did not accumulate in the ER but was targeted to the vacuole. They concluded that prolamin retention in the ER of endosperm cells of wheat may result from their aggregation. This discrepancy with the present results could be due to the higher expression level of the construct used here, where a double 35S promoter was used compared with a single 35S promoter by Napier *et al.* (1997). Thus in the present experiments, the high expression level could explain the accumulation of γ-gliadin and its transient retention in the ER before trafficking to vacuoles. Alternatively, it is also possible that ER retention and PBLS formation observed with the N- and C-terminal γ-gliadin domains could be driven by totally different mechanisms. One of them could be due to the repeated sequence and membrane anchor as suggested (Banc *et al.*, 2009), and the second mechanism could involve intramolecular disulphide bond formation between the cysteines of γ-gliadin, which play a major role in the conformation of the gliadins and also control their accumulation as proposed previously

(Shimoni and Galili, 1996). Moreover, in contrast to the isolated N-terminal domain, the isolated C-terminal domain of γ-gliadin is insoluble in aqueous solution (Altschuler *et al.*, 1993; data not shown), so its ER retention and accumulation could be due to its aggregation in relation to its insolubility. Under this hypothesis the ER retention and accumulation observed with full-length γ-gliadin could result from the combination of these different mechanisms, but this remains to be proven. It was also shown that both domains of γ-gliadin are able to interact in an *in vitro* yeast-two hybrid assay, which was confirmed *in planta* by a FRET-FLIM assay. The interaction between these domains could also be an important element involved in the global mechanism of prolamin ER retention. Other studies remain to be performed in order to explore this question further, particularly the determination of the interactions between all wheat prolamins, that is gliadins and glutenins, and the analysis of their distribution within PBs.

Through stable expression in BY-2 cells, it was demonstrated that γ-gliadin and both its domains fused to GFP were transported to and accumulated in vacuoles after being retained in the ER for several days. It was demonstrated that this process was Golgi dependent since BFA treatment prevented the vacuolar delivery. This was also the case when γ-gliadin was expressed in tobacco plants (Napier *et al.*, 1997). Moreover, immunoblotting revealed that gliadin–GFP which escaped the ER underwent a degradation process, since a 27 kDa GFP band was dominant during the stationary phase of cell growth. It was shown that the fusion of GFP with the γ-zein domain involved in polymerization of zein, the maize storage protein, also undergoes vacuolar sorting, indicating a protein quality control pathway for degradation in the plant vacuole (Foresti *et al.*, 2008).

ER quality control occurs when proteins are not correctly folded in the ER, termed ERAD (ER-associated degradation) that involves retrotranslocation from the ER into the cytosol and degradation by the proteasome (Anelli and Sitia 2008). Also in some cases, polypeptides form aggregates in the ER that can be disposed of by autophagy of portions of the ER as demonstrated with the yeast system (Kruse *et al.*, 2006). In maturing seeds, storage proteins are synthesized in the ER where they are trapped by BiP to form aggregates. These aggregates can be transported to protein storage vacuoles via autophagic bodies or in specific instances by precursor-accumulating vesicles (PACs) (Levanony *et al.*, 1992; Hara-Nishimura *et al.*, 1998, respectively). The present results suggest that in BY-2 cells gliadin–GFP, after being retained in the ER, is transported to and degraded in vacuoles. This trafficking pathway could be unrelated to the process existing in the wheat endosperm cells, since in this latter case the aggregates transported are not intended for degradation in endosperm cells, in contrast to the present observations in BY-2 cells. In addition, few PBLS were observed in stable transgenic BY-2 lines compared with the transient tobacco leaf system, which could suggest that this vacuolar delivery could be independent of PBLS formation as previously mentioned for other ER residents (Tamura *et al.*, 2004). However, the increase in size of the PBLS during BFA treatment reinforces the argument previously suggested with the transient tobacco leaf system, that the increase in size of PBLS is due to coalescence of smaller bodies within the ER to form larger PBLS over longer periods of expression.

The involvement of the ER chaperone BiP in the delivery of proteins to the vacuole in a Golgi-dependent manner was recently demonstrated (Pimpl *et al.*, 2006). This BiP-mediated vacuolar process could act in addition to ERAD to maximize the efficiency of quality control in the secretory pathway. It would be interesting to determine the involvement of BiP in the PB formation and trafficking pathway, and to determine the involvement of ERAD or alternative post-ER quality control actors in the transport pathway of wheat prolamins in tobacco model and wheat endosperm cells.

In conclusion, the expression of γ-gliadin fluorescent protein fusions in tobacco cells proved to be a useful model to investigate the mechanisms involved in the unconventional protein trafficking pathway followed by seed storage prolamins. Studies with other wheat prolamins such as high and low molecular weight glutenin should now be carried out to elucidate further the trafficking pathway of wheat seed storage prolamins, taking into account their polymorphism and structural complexity.

Supplementary data

Supplementary data are available at *JXB* online.

Supplementary Movie S1. γ-Gliadin protein body-like structures (γ-gliadin–GFP in green) moved throughout the cell along the ER network (mRFP–ER marker in magenta).

Supplementary Movie S2. γ-Gliadin protein body-like structures (γ-gliadin–GFP in green) are not co-localized with Golgi bodies (ST–mRFP in magenta).

Supplementary Movie S3. The C-terminal domain of γ-gliadin (Cter-γ-gliadin–GFP in green) forms protein body-like structures which moved throughout the cell along the ER network (mRFP–ER marker in magenta).

Supplementary Movie S4. N-terminal domain of γ-gliadin (Nter-γ-gliadin–mRFP in magenta) forms protein body-like structures, the majority of which are mobile and are associated with the ER network (GFP–ER marker in green).

Acknowledgements

References

Anelli T, Sitia R. 2008. Protein quality control in the early secretory pathway. *EMBO Journal* **27,** 315–327.

Altschuler Y, Rosenberg N, Harel R, Galili G. 1993. The N- and C-terminal regions regulate the transport of wheat γ-gliadin through the endoplasmic reticulum in Xenopus oocytes. *The Plant Cell* **5,** 443–450.

Banc A, Desbat B, Renard D, Popineau Y, Mangavel C, Navailles L. 2009. Exploring the interactions of gliadins with model membranes: effect of confined geometry and interfaces. *Biopolymers* **91,** 610–622.

Bellucci M, Alpini A, Paolocci F, Cong L, Arcioni S. 2000. Accumulation of maize gamma-zein and gamma-zein:KDEL to high levels in tobacco leaves and differential increase of BiP synthesis in transformants. *Theoretical and Applied Genetics* **101,** 796–804.

Conley AJ, Joensuu JJ, Menassa R, Brandle JE. 2009. Induction of protein body formation in plant leaves by elastin-like polypeptide fusions. *BMC Biology* **7,** 48.

Curtis MD, Grossniklaus U. 2003. A gateway cloning vector set for high-throughput functional analysis of genes in planta. *Plant Physiology* **133,** 462–469.

De Virgilio M, De Marchis F, Bellucci M, Mainieri D, Rossi M, Benvenuto E, Arcioni S, Vitale A. 2008. The human immunodeficiency virus antigen Nef forms protein bodies in leaves of transgenic tobacco when fused to zeolin. *Journal of Experimental Botany* **59,** 2815–2829.

Foresti O, De Marchis F, de Virgilio M, Klein EM, Arcioni S, Bellucci M, Vitale A. 2008. Protein domains involved in assembly in the endoplasmic reticulum promote vacuolar delivery when fused to secretory GFP, indicating a protein quality control pathway for degradation in the plant vacuole. *Molecular Plant* **1,** 1067–1076.

Galili G, Altschuler Y, Levanony H. 1993. Assembly and transport of seed storage proteins. *Trends in Cell Biology* **3,** 437–442.

Geli MI, Torrent M, Ludevid D. 1994. Two structural domains mediate two sequential events in γ-zein targeting: protein endoplasmic reticulum retention and protein body formation. *The Plant Cell* **6,** 1911–1922.

Gomord V, Fitchette AC, Denmat LA, Michaud D, Faye L. 1998. Production of foreign proteins in tobacco cell suspension culture. In: Cunningham C, Porter AJR, eds. *Methods in molecular biotechnology*, Vol. 3. Totowa, NJ: Humana Press, 155–164.

Hara-Nishimura II , Shimada T, Hatano K, Takeuchi Y, Nishimura M. 1998. Transport of storage proteins to protein storage vacuoles is mediated by large precursor-accumulating vesicles. *The Plant Cell* **10,** 825–836.

Karimi M, De Meyer B, Hilson P. 2005. Modular cloning in plant cells. *Trends in Plant Science* **10,** 103–105.

Kogan MJ, López O, Cocera M, López-Iglesias C, De La Maza A, Giralt E. 2004. Exploring the interaction of the surfactant N-terminal domain of gamma-zein with soybean phosphatidylcholine liposomes. *Biopolymers* **73,** 258–268.

Kotzer AM, Brandizzi F, Neumann U, Paris N, Moore I, Hawes C. 2004. AtRabF2b (Ara7) acts on the vacuolar trafficking pathway in tobacco leaf epidermal cells. *Journal of Cell Science* **117,** 6377–6389.

Kruse KB, Brodsky JL, McCracken AA. 2006. Autophagy: an ER protein quality control process. *Autophagy* **2,** 135–137.

Levanony H, Rubin R, Altschuler Y, Galili G. 1992. Evidence for a novel route of wheat storage proteins to vacuoles. *Journal of Cell Biology* **119,** 1117–1128.

Loussert C, Popineau Y, Mangavel C. 2008. Protein bodies ontogeny and localization of prolamin components in the developing endosperm of wheat caryopses. *Journal of Cereal Science* **47,** 445–456.

Mainieri D, Rossi M, Archinti M, Bellucci M, De Marchis F, Vavassori S, Pompa A, Arcioni S, Vitale A. 2004. Zeolin. A new recombinant storage protein constructed using maize gamma-zein and bean phaseolin. *Plant Physiology* **136,** 3447–3456.

Marion J, Bach L, Bellec Y, Meyer C, Gissot L, Faure JD. 2008. Systematic analysis of protein subcellular localization and interaction using high-throughput transient transformation of Arabidopsis seedlings. *The Plant Journal* **56,** 169–179.

Maruyama N, Okuda E, Tatsuhara M, Utsumi S. 2008. Aggregation of proteins having Golgi apparatus sorting determinant induces large globular structures derived from the endoplasmic reticulum in plant seed cells. *FEBS Letters* **582,** 1599–1606.

Muench DG, Wu Y, Zhang Y, Li X, Boston RS, Okita TW. 1997. Molecular cloning, expression and subcellular localization of a BiP homolog from rice endosperm tissue. *Plant and Cell Physiology* **38,** 404–412.

Napier RM, Fowke LC, Hawes C, Lewis M, Pelham HR. 1992. Immunological evidence that plants use both HDEL and KDEL for targeting proteins to the endoplasmic reticulum. *Journal of Cell Science* **102,** 261–271.

Napier JA, Richard G, Turner MF, Shewry PR. 1997. Trafficking of wheat gluten proteins in transgenic tobacco plants: gamma-gliadin does not contain an endoplasmic reticulum retention signal. *Planta* **203,** 488–494.

Parker ML. 1982. Protein accumulation in developing endosperm of a high-protein line of Triticum dicoccoides. *Plant, Cell and Environnment* **5,** 37–43.

Parker ML, Hawes CR. 1982. The Golgi-apparatus in developing endosperm of wheat (*Triticum aestivum* L). *Planta* **154,** 277–283.

Pimpl P, Taylor JP, Snowden C, Hillmer S, Robinson DG, Denecke J. 2006. Golgi-mediated vacuolar sorting of the endoplasmic reticulum chaperone BiP may play an active role in quality control within the secretory pathway. *The Plant Cell* **18,** 198–211.

Pompa A, Vitale A. 2006. Retention of a bean phaseolin/maize gamma-Zein fusion in the endoplasmic reticulum depends on disulfide bond formation. *The Plant Cell* **18,** 2608–2621.

Rosenberg N, Shimoni Y, Altschuler Y, Levanony H, Volokita M, Galili G. 1993. Wheat (*Triticum aestivum* L.) γ-gliadin accumulates in dense protein bodies within the endoplasmic reticulum of yeast. *Plant Physiology* **102,** 61–69.

Rubin R, Levanony H, Galili G. 1992. Evidence for the presence of two different types of protein bodies in wheat endosperm. *Plant Physiology* **99,** 718–724.

Saito Y, Kishida K, Takata K, Takahashi H, Shimada T, Tanaka K, Morita S, Satoh S, Masumura T. 2009. A green fluorescent protein fused to rice prolamin forms protein body-like structures in transgenic rice. *Journal of Experimental Botany* **60,** 615–627.

Shewry PR, Halford NG. 2002. Cereal seed storage proteins: structures, properties and role in grain utilization. *Journal of Experimental Botany* **53,** 947–958.

Shewry PR, Napier JA, Tatham AS. 1995. Seed storage proteins: structures and biosynthesis. *The Plant Cell* **7,** 945–956.

Shimoni Y, Galili G. 1996. Intramolecular disulfide bonds between conserved cysteines in wheat gliadins control their deposition into protein bodies. *Journal of Biological Chemistry* **271,** 18869–18874.

Shy G, Ehler L, Herman E, Galili G. 2001. Expression patterns of genes encoding endomembrane proteins support a reduced function of the Golgi in wheat endosperm during the onset of storage protein deposition. *Journal of Experimental Botany* **52,** 2387–2388.

Sparkes I, Frigerio L, Tolley N, Hawes C. 2009*b*. The plant endoplasmic reticulum: a cell wide web. *Biochemical Journal* **423,** 145–155.

Sparkes I, Runions J, Hawes C, Griffing L. 2009*a*. Movement and remodelling of the endoplasmic reticulum in nondividing cells of tobacco leaves. *The Plant Cell* **21,** 3937–3949.

Sparkes IA, Runions J, Kearns A, Hawes C. 2006. Rapid, transient expression of fluorescent fusion proteins in tobacco plants and generation of stably transformed plants. *Nature Protocols* **1,** 2019–2025.

Sparkes I, Tolley N, Aller I, Svozil J, Osterrieder A, Botchway S, Mueller C, Frigerio L, Hawes C. 2010. Five *Arabidopsis* reticulon isoforms share endoplasmic reticulum location, topology, and membrane shaping properties. *The Plant Cell* **22,** 1333–1343.

Tamura K, Shimada T, Ono E, Tanaka Y, Nagatani A, Higashi SI, Watanabe M, Nishimura M, Hara-Nishimura I. 2003. Why green fluorescent fusion proteins have not been observed in the vacuoles of higher plants. *The Plant Journal* **35,** 545–555.

Tamura K, Yamada K, Shimada T, Hara-Nishimura I. 2004. Endoplasmic reticulum-resident proteins are constitutively transported to vacuoles for degradation. *The Plant Journal* **39,** 393–402.

Tatham AS, Masson P, Popineau Y. 1990. Conformational studies of peptides derived by the enzymic hydrolysis of a gamma-type gliadin. *Journal of Cereal Science* **11,** 1–13.

Torrent M, Geli MI, Ruiz-Avila L, Canals JM, Puigdomènech P, Ludevid D. 1994. Role of structural domains for maize gamma-zein retention in Xenopus oocytes. *Planta* **192,** 512–518.

Torrent M, Llompart B, Lasserre-Ramassamy S, *et al*. 2009. Eukaryotic protein production in designed storage organelles. *BMC Biology* **7,** 5.

Tosi P, Parker M, Gritsch CS, Carzaniga R, Martin B, Shewry PR. 2009. Trafficking of storage proteins in developing grain of wheat. *Journal of Experimental Botany* **60,** 979–991.

Vitale A, Ceriotti A. 2004. Protein quality control mechanisms and protein storage in the endoplasmic reticulum. A conflict of interests? *Plant Physiology* **136,** 3420–3426.

Vitale A, Galili G. 2001. The endomembrane system and the problem of protein sorting. *Plant Physiology* **125,** 115–118.

Vitale A, Hinz G. 2005. Sorting of proteins to storage vacuoles: how many mechanisms? *Trends in Plant Science* **10,** 316–323.